

**Anomalous 2D-Confined Electronic Transport in Layered Organic Charge-Glass Systems**Takuro Sato<sup>1,\*</sup>, Kazuya Miyagawa<sup>1</sup>, Masafumi Tamura<sup>2</sup>, and Kazushi Kanoda<sup>1,†</sup><sup>1</sup>*Department of Applied Physics, University of Tokyo, Tokyo 113-8656, Japan*<sup>2</sup>*Department of Physics, Faculty of Science and Technology, Tokyo University of Science, Noda, Chiba 278-8510, Japan*

(Received 9 April 2020; accepted 9 September 2020; published 30 September 2020)

To get insight into the nature of the electronic fluid in the frustration-driven charge glasses, we investigate in-plane and out-of-plane charge transport for several quasitriangular-lattice organic systems:  $\theta$ -(BEDT-TTF)<sub>2</sub>X [ $X = \text{RbZn}(\text{SCN})_4$ ,  $\text{CsZn}(\text{SCN})_4$ , and  $\text{I}_3$ ]. These compounds host a charge order, charge glass, and Fermi liquid, depending on the strength of the charge frustration. We find that the resistivity exhibits extreme 2D anisotropy and contrasting temperature dependence between the in-plane and out-of-plane directions in the charge-glass phase, unlike in the charge order and metallic states. The experimental features indicate that the frustration-induced charge glass carries an anomalous 2D-confined electronic fluid with possible charge excitations other than conventional quasiparticles.

DOI: 10.1103/PhysRevLett.125.146601

A glass state of electrons that does not originate in disorder, i.e., a charge-glass (CG) state, arises from frustration in Coulomb interactions on triangularlike lattices [1–5] in a manner similar to frustrated spin systems [6–8] and is conceptually distinguished from conventional electronic inhomogeneity as caused by randomly located dopants [9–11]. The CG was demonstrated in layered organic conductors with quasitriangular lattices [12–16] through observing a charge inhomogeneity [16,17], an exponential slowing down of electron dynamics [12,13], and ergodicity breaking signified by the cooling-rate dependence and aging of resistivity [13] as well as the electronic crystallization from glass [16,18]. All of these observations are hallmark properties of glasses [19–21].

The organic materials,  $\theta$ -(BEDT-TTF)<sub>2</sub>X (BEDT-TTF denotes bis(ethylenedithio)tetrathiafulvalene), have conducting layers in which BEDT-TTFs form isosceles triangular lattices dubbed  $\theta$  type and accommodate a hole per two molecules and insulating X (anion) layers [22,23] [Fig. 1(a)]. A strong Coulomb repulsion,  $V$ , between the neighboring molecular sites generally stabilizes a charge order (CO) [24] but does not do so on the isosceles triangular lattices [25–27]. The ratio of two intersite Coulomb energies,  $V_p/V_c$ , a measure of charge frustration [Fig. 1(b)], is systematically varied with X as 0.87, 0.91, and 0.95 for  $X = \text{RbZn}(\text{SCN})_4$ ,  $\text{CsZn}(\text{SCN})_4$ , and  $\text{I}_3$  (hereafter abbreviated as  $\theta$ -RbZn,  $\theta$ -CsZn, and  $\theta$ -I<sub>3</sub>), respectively [Fig. 1(c)] [28,29]. Such a tiny perturbation of the frustration results in a remarkable change in electronic states, which is in line with a widely accepted notion in a field of classical glass [30].

The least frustrated  $\theta$ -RbZn exhibits a first-order transition into a horizontal stripe CO from a charge liquid (CL) at 200 K when cooled slowly at a rate of less than  $\sim 5$  K/min; however, a faster cooling suppresses the CO

transition and gives a smooth pathway from the CL to the CG [12,31,32].  $\theta$ -CsZn does not exhibit the transition to the CO even when cooled slowly, e.g., at 0.1 K/min, but instead shows a continuous change from a CL to the CG in a manner similar to the rapidly cooled  $\theta$ -RbZn [13,33,34]. Interestingly, the most frustrated system,  $\theta$ -I<sub>3</sub>, in which a quantum nature suppresses the CO and/or CG in a critical manner falls into a Fermi liquid (FL) instead of CG at low temperatures, which is theoretically ascribable to a frustration-driven quantum melting of CG [35–38]. The FL crosses over at high temperatures to a kind of CL [39] distinguished from the CL in  $\theta$ -RbZn and  $\theta$ -CsZn in resistivity fluctuations and x-ray diffuse scattering [35]; the nature of CL differs whether it falls into a CG or a FL at low temperatures. The electronic states in these  $\theta$ -(BEDT-TTF)<sub>2</sub>X systems are summarized by a conceptual phase diagram regarding the geometrical frustration [Fig. 1(c)].

The CG shares the universal features of conventional classical glasses but raises a significant issue connected to the quantum nature of electrons. The resistivity of the CG is weakly temperature-dependent, even metallic in  $\theta$ -CsZn, and several orders of magnitude smaller than that of the CO. Obviously, a naïve picture of the CG, a glassy freezing of electron dynamics that should lead to the localization of electrons, does not hold in the real CG. The puzzling transport behavior is sure to be a key to the nature of the glass formed by the quantum particles: electrons.

Here, we investigate in-plane and out-of-plane resistivities for  $\theta$ -RbZn,  $\theta$ -CsZn, and  $\theta$ -I<sub>3</sub> to characterize the fluidity of the CG in view of anisotropy, expecting that unusual charge excitations, if any, manifest themselves in directional dependence of transport characteristics as revealed in strongly correlated electron systems [40,41]. A conventional metal-to-CO transition system,

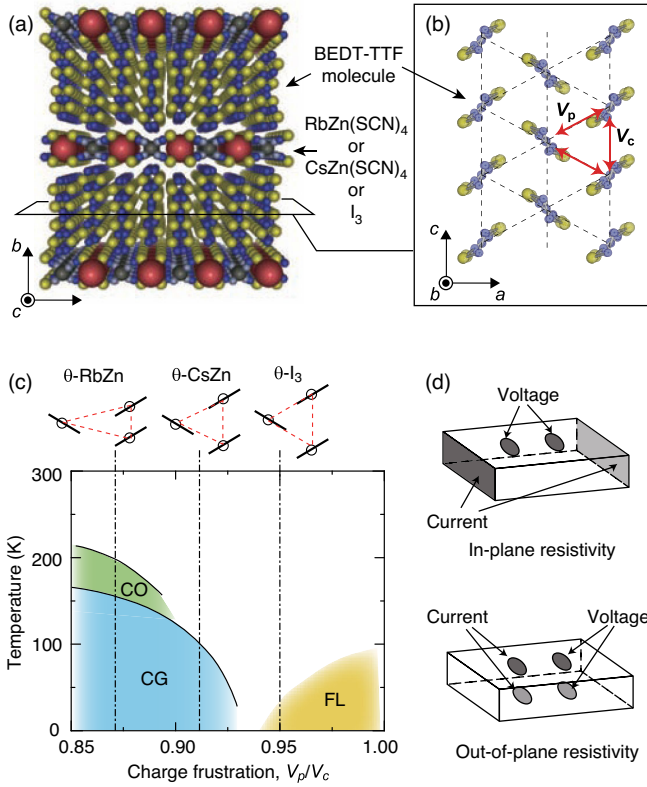


FIG. 1. (a) Crystal structure of  $\theta$ -(BEDT-TTF) $_2$ X system. Conducting BEDT-TTF layers and insulating anion ones are stacked along the  $b$  axis. Note that the crystal structure shown here is for  $\theta$ -RbZn and  $\theta$ -CsZn, and the long axis of the BEDT-TTF molecules in  $\theta$ -I $_3$  and  $\alpha$ -I $_3$  tilts slightly from the out-of-plane direction. (b) Molecular arrangement in conducting layers in which BEDT-TTF molecules form an anisotropic triangular lattice. (c) Schematic phase diagram for  $\theta$ -(BEDT-TTF) $_2$ X in terms of charge frustration. CO, CG, and FL represent the charge-order, charge-glass, and Fermi-liquid states, respectively. (d) Configurations of current and voltage terminals for the present resistivity measurements.

$\alpha$ -(BEDT-TTF) $_2$ I $_3$  (hereafter abbreviated as  $\alpha$ -I $_3$ ) [42,43], was also investigated as a reference of the frustration-free system. We found that the charge transport in the CG state is anomalously confined to 2D layers.

Single crystals of  $\theta$ -RbZn,  $\theta$ -CsZn,  $\theta$ -I $_3$ , and  $\alpha$ -I $_3$  were synthesized by the galvanostatic anodic oxidation of BEDT-TTF as described in the literature [22,23]. Both the in-plane and out-of-plane resistivities were measured by the four-terminal method with the electrode configurations shown in Fig. 1(d); the in-plane resistivity was measured with the current contacts attached on the entire sides of a crystal to ensure a uniform current flow in the crystal, whereas the out-of-plane resistivity could be precisely measured with the conventional contacts of electrodes [Fig. 1(d)] thanks to a huge anisotropy of resistivity.

Figure 2 shows the temperature dependence of out-of-plane resistivity  $\rho_{\perp}$  and in-plane resistivity  $\rho_{\parallel}$  for the four

systems. Abrupt increases in  $\rho_{\perp}$  and  $\rho_{\parallel}$  at 200 K for  $\theta$ -RbZn in a slowly cooled condition (0.2 K/min) indicate a transition from CL to CO, which is suppressed by rapid cooling (4 K/min) and gives way to a smooth change from CL to CG [Fig. 2(a)] in a manner similar to the behavior observed in  $\theta$ -CsZn irrespective of the cooling rate [Fig. 2(b)]. The nominal CL to CG transition temperature,  $T_g$ , is 160–170 K for  $\theta$ -RbZn [12] and 100 K for  $\theta$ -CsZn [13] as the onsets of the ergodicity breaking; note that the  $T_g$  has no thermodynamic sense here but defines a phenomenological temperature at which the dynamics slows down to the laboratory timescale, e.g.,  $10^2$  s.  $\theta$ -I $_3$  is metallic in the entire temperature range [Fig. 2(c)], and  $\alpha$ -I $_3$  shows a clear first-order CO transition both in  $\rho_{\perp}$  and  $\rho_{\parallel}$  at 135 K [Fig. 2(d)]. A prominent feature of the CG states in  $\theta$ -RbZn and  $\theta$ -CsZn is a remarkable temperature dependence of an anisotropy ratio  $\rho_{\perp}/\rho_{\parallel}$ . As the temperature is lowered,  $\rho_{\perp}/\rho_{\parallel}$  steeply increases more than one or two orders of magnitude up to the range of  $10^6 - 10^7$  commonly for  $\theta$ -RbZn and  $\theta$ -CsZn, strongly pointing to highly 2D electronic states in the CG [Fig. 3(a),(b)]. We note a previous x-ray study for an analogous material,  $\theta$ -CsCo, that has revealed that the out-of-plane lattice constant shortens by 0.5% on cooling from 300 K to 20 K [44]; it works for the out-of-plane transport to become more conductive on cooling, contradicting the observation.

The extraordinarily large values of  $\rho_{\perp}/\rho_{\parallel}$  in CG and its anomalous temperature evolution from CL to CG are highlighted with reference to the behavior of the metallic  $\theta$ -I $_3$ , the CO state in  $\theta$ -RbZn, and the nonfrustrated  $\alpha$ -I $_3$ . In  $\theta$ -I $_3$ ,  $\rho_{\perp}/\rho_{\parallel}$  is  $3 \times 10^3$  at room temperature and moderately decreases with temperature to below  $1 \times 10^3$  in the FL regime [Fig. 3(c)], where both  $\rho_{\parallel}$  and  $\rho_{\perp}$  vary in proportion to the squared temperature [inset in Fig. 2(c)]. In the CO state of  $\theta$ -RbZn,  $\rho_{\perp}/\rho_{\parallel}$  falls into the range of  $10^3$  and is, more importantly, much less temperature-dependent than in the CG [Fig. 3(b)]. Remarkably, the temperature-invariant  $\rho_{\perp}/\rho_{\parallel}$  is also the case to the  $\alpha$ -I $_3$  even across the metal-to-CO transition, and the value of  $\rho_{\perp}/\rho_{\parallel}$  in  $\alpha$ -I $_3$  is comparable to that of  $\theta$ -I $_3$  and the CO state of  $\theta$ -RbZn [Fig. 3(d)]. We particularly emphasize that the increase of  $\rho_{\perp}/\rho_{\parallel}$  by orders of magnitude in the CG has no explanation in terms of quasiparticles in either metals or insulators. Thus, the electron transport strongly confined to the 2D layers is specific to the CG. We note that, in  $\theta$ -CsZn, an increase in  $\rho_{\perp}/\rho_{\parallel}$  on cooling turns to a decrease at the lowest temperatures [Fig. 3(b)], coinciding with steep increases in both  $\rho_{\perp}$  and  $\rho_{\parallel}$  [Fig. 2(b)]. This is likely related to the CO seeds growing in size ( $\sim 60$  Å at 5 K) and fraction as signified by the x-ray diffuse scattering of  $(0, k, 1/2)$  at low temperatures [13,45].

The noticeable temperature dependence of  $\rho_{\perp}/\rho_{\parallel}$  means that  $\rho_{\perp}$  and  $\rho_{\parallel}$  vary differently with temperature.  $\theta$ -RbZn is nonmetallic in both  $\rho_{\perp}$  and  $\rho_{\parallel}$ , and thus their behaviors are examined with the activation plots in Fig. 4. In the CL-CG

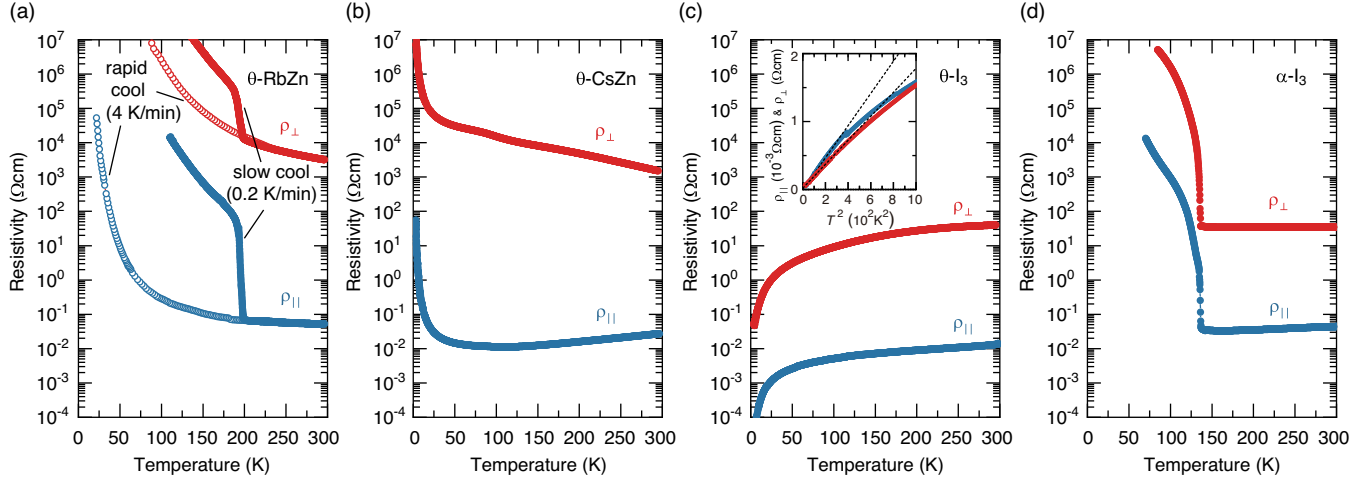


FIG. 2. Temperature dependencies of in-plane (blue) and out-of-plane (red) resistivities for (a)  $\theta$ -RbZn, (b)  $\theta$ -CsZn, (c)  $\theta$ -I<sub>3</sub>, and (d)  $\alpha$ -I<sub>3</sub>. Open and closed circles in (a) represent the resistivities measured with rapid (4 K/min) and slow (0.2 K/min) cooling, respectively. The inset in (c) displays in-plane and out-of-plane resistivities against  $T^2$  for  $\theta$ -I<sub>3</sub>.

state, the temperature dependence of  $\rho_{\perp}$  is well described by an Arrhenius function with an activation energy,  $\Delta$ , of  $\sim 1000$  K in the form of  $\rho_{\perp} \propto e^{\Delta/T}$ , whereas  $\rho_{\parallel}$  is characterized by  $\Delta \sim 300$  K at the low-temperature part (Fig. 4), indicating the strong suppression of the out-of-plane charge transport. We note that, in the CO state,  $\rho_{\parallel}$  and  $\rho_{\perp}$  show a similar activation behavior with  $\Delta \sim 1300$  K and 1400 K, respectively, signifying no 2D confinement (inset in Fig. 4). The contrasting temperature dependence of  $\rho_{\parallel}$  and  $\rho_{\perp}$  in the CL-CG state is particularly marked in  $\theta$ -CsZn, where  $\rho_{\parallel}$  behaves as a metallic, whereas  $\rho_{\perp}$  is nonmetallic in temperatures of 100–300 K; the highly conductive in-plane charge transport is prohibited in the out-of-plane direction.

The CL and CG in  $\theta$ -RbZn exhibit short-ranged CO domains with a wave vector of  $\mathbf{q}_1[\sim(\pm 1/3, k, \pm 1/4)]$  ( $k$  denotes negligible coherence between the BEDT-TTF layers) [12,46]. Theoretically, the long-ranged CO with the  $\mathbf{q}_1$  is stabilized by a strong charge frustration on triangular lattices and retains a metallic state [26,47]. In reality, the  $\mathbf{q}_1$  modulation is not long-ranged but short-ranged  $\mathbf{q}_1$  domains are formed, which simultaneously cause glass-forming behavior and the itinerancy of electrons. Note that the charge domains have no correlation between the adjacent layers [48], which should be partly responsible for the extremely 2D nature of the charge transport. The contrasting temperature dependencies of  $\rho_{\parallel}$  and  $\rho_{\perp}$ , metallic vs nonmetallic as observed in  $\theta$ -CsZn, may signal the

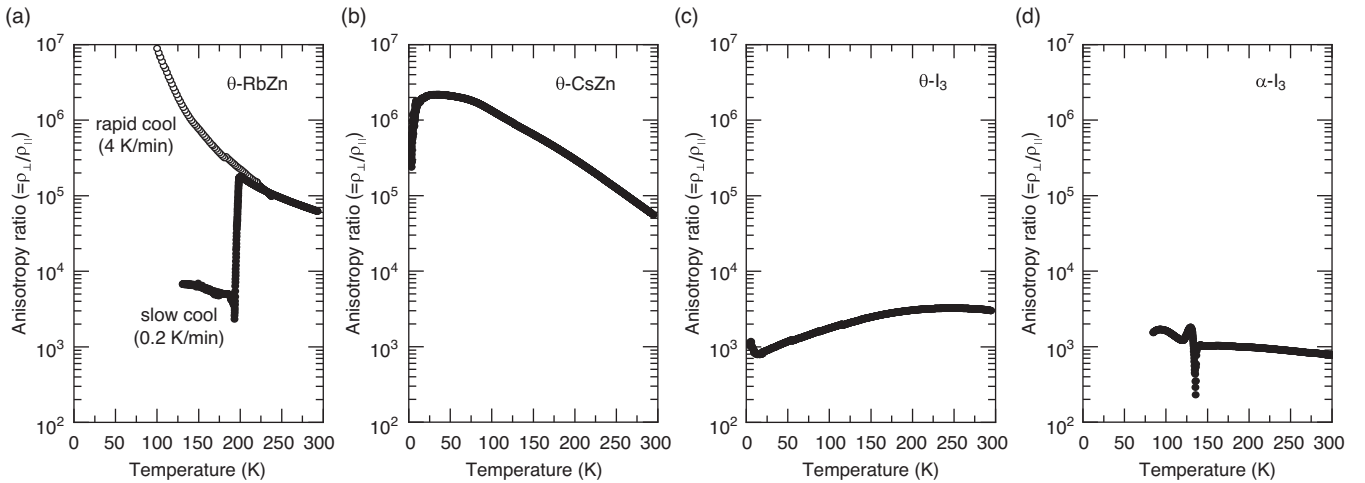


FIG. 3. Temperature dependencies of anisotropy ratios  $\rho_{\perp}/\rho_{\parallel}$  for (a)  $\theta$ -RbZn, (b)  $\theta$ -CsZn, (c)  $\theta$ -I<sub>3</sub>, and (d)  $\alpha$ -I<sub>3</sub>. Each profile is deduced from the results in Fig. 2. Open and closed circles in (a) represent the resistivities measured with rapid (4 K/min) and slow (0.2 K/min) cooling, respectively.

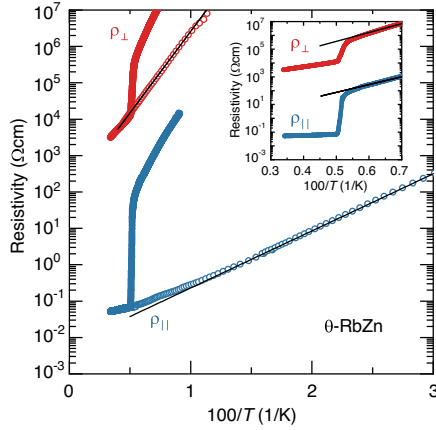


FIG. 4. The in-plane (blue) and out-of-plane (red) resistivities for  $\theta$ -RbZn against the inverse of temperature. Open and closed circles represent the data acquired in the rapid-cooled (4 K/min) and slow-cooled (0.2 K/min) conditions, respectively. The inset shows an enlarged figure around the CL state. The black lines are the resultant fitting curves by Arrhenius-type function.

unconventional natures of low-energy charge excitations underlying their 2D confinement. In a conventional metal or semiconductor, which postulates quasiparticles as elementary charge excitations, the temperature dependence of out-of-plane conductivity should be generally similar to that of in-plane [41,49,50]. Indeed, we found temperature-insensitive  $\rho_{\perp}/\rho_{\parallel}$  in the  $\theta$ -I<sub>3</sub>, the CO state in  $\theta$ -RbZn, and the nonfrustrated  $\alpha$ -I<sub>3</sub>. Therefore, the significant temperature evolution of  $\rho_{\perp}/\rho_{\parallel}$  or the qualitative discrepancy between the temperature profiles of  $\rho_{\parallel}$  and  $\rho_{\perp}$  in the CL-CG state is difficult to reconcile with a conventional quasiparticle picture. The possible breakdown of the quasiparticle picture is also consistent with the fact that the metallic  $\rho_{\parallel}$  exceeds the value of  $\sim 1$  m $\Omega$  cm deduced from  $k_F l \sim 1$  with  $l$  the lattice spacing, the so-called Mott-Ioffe-Regel limit for the quasiparticle transport [39].

The 2D confinement of the charge transport is reminiscent of the similar behavior of the underdoped high- $T_c$  copper oxides, in which charge and spin excitations are separated in the 2D conducting layers and hardly hop between the layers with the separated degrees of freedom retained. It is intriguing if the separation or fractionalization of electron degrees of freedom or some collective excitations unable to directly hop to adjacent layers are associated with the 2D confined charge excitations; further insights await theoretical investigations. We note that temperature evolutions of  $\rho_{\perp}$  not in parallel with  $\rho_{\parallel}$  are argued in terms of a strong coupling of electrons with phonons propagating in the out-of-plane direction, leading to a formation of polarons [51]. This scenario expects a factorial increase in the resistivity anisotropy and a substantial maximum in  $\rho_{\perp}$  around the Debye temperature, however, which appears to conflict with the more than 2 orders of magnitude increase of the anisotropy and the absence of peaks in  $\rho_{\perp}$  (Fig. 2).

Apparently, the in-plane itinerancy of electrons in CG contradicts the classical dynamics or freezing in glass; how do they reconcile with each other? As indicated by NMR spectra in  $\theta$ -RbZn and  $\theta$ -CsZn [16,17,52], the charge of the molecular site in the CG and CL states is distributed continuously in magnitude, indicating that the inhomogeneous entity responsible for the classical glass dynamics is the interaction-induced emergent “charge density” instead of individual electrons. Specific to the present systems, threefold charge density modulations reconcile with itinerant electrons [26,47,53], and the itinerancy is likely retained even when the threefold modulation is short-ranged and takes on a glassy feature due to the charge frustration. The classical glass dynamics of the charge density should be reflected in the behavior of the itinerant fluid through their coupling. It is theoretically suggested that itinerant fermions with long-range interactions can form a glass state, dubbed a quantum charge glass [54]. There is a general belief in the physics of soft matter that the hierarchical structure underlies the properties of conventional glass systems [55,56]. We suggest that the electronic counterpart of the conventional glass adds the conceptually novel “quantum-classical energetic hierarchy” to the physics of glass. The present results reveal highly unconventional low-energy excitations, which are strongly 2D confined and possibly distinct from the conventional quasiparticles, in the novel glass systems retaining quantum nature.

This work was supported in part by the Japan Society for the Promotion of Science (JSPS) KAKENHI (Grant Nos. 25220709, 17K05532, 18H05225, and 19H01846). T.S. was supported as a JSPS Research Fellow (No. 14J07870).

\*Corresponding author.  
takuro.sato@riken.jp

†Corresponding author.  
kanoda@ap.t.u-tokyo.ac.jp

- [1] P. W. Anderson, *Phys. Rev.* **102**, 1008 (1956).
- [2] S. Mahmoudian, L. Rademaker, A. Ralko, S. Fratini, and V. Dobrosavljević, *Phys. Rev. Lett.* **115**, 025701 (2015).
- [3] L. Rademaker, Z. Nussinov, L. Balents, and V. Dobrosavljević, *New J. Phys.* **20**, 043026 (2018).
- [4] L. Rademaker, A. Ralko, S. Fratini, and V. Dobrosavljević, *J. Supercond. Novel Magn.* **29**, 601 (2016).
- [5] K. Yoshimi and H. Maebashi, *J. Phys. Soc. Jpn.* **81**, 063003 (2012).
- [6] Y. Shimizu, K. Miyagawa, K. Kanoda, M. Maesato, and G. Saito, *Phys. Rev. Lett.* **91**, 107001 (2003).
- [7] L. Balents, *Nature (London)* **464**, 199 (2010).
- [8] Y. Zhou, K. Kanoda, and T.-K. Ng, *Rev. Mod. Phys.* **89**, 025003 (2017).
- [9] E. Dagotto, *Science* **309**, 257 (2005).
- [10] I. Zeljkovic, Z. Xu, J. Wen, G. Gu, R. S. Markiewicz, and J. E. Hoffman, *Science* **337**, 320 (2012).

- [11] S. Bogdanovich and D. Popović, *Phys. Rev. Lett.* **88**, 236401 (2002).
- [12] F. Kagawa, T. Sato, K. Miyagawa, K. Kanoda, Y. Tokura, K. Kobayashi, R. Kumai, and Y. Murakami, *Nat. Phys.* **9**, 419 (2013).
- [13] T. Sato, F. Kagawa, K. Kobayashi, K. Miyagawa, K. Kanoda, R. Kumai, Y. Murakami, and Y. Tokura, *Phys. Rev. B* **89**, 121102(R) (2014).
- [14] T. Sato, F. Kagawa, K. Kobayashi, A. Ueda, H. Mori, K. Miyagawa, K. Kanoda, R. Kumai, Y. Murakami, and Y. Tokura, *J. Phys. Soc. Jpn.* **83**, 083602 (2014).
- [15] T. Sato, K. Miyagawa, and K. Kanoda, *J. Phys. Soc. Jpn.* **85**, 123702 (2016).
- [16] T. Sato, K. Miyagawa, and K. Kanoda, *Science* **357**, 1378 (2017).
- [17] R. Chiba, K. Hiraki, T. Takahashi, H. M. Yamamoto, and T. Nakamura, *Phys. Rev. B* **77**, 115113 (2008).
- [18] S. Sasaki, K. Hashimoto, R. Kobayashi, K. Itoh, S. Iguchi, Y. Nishio, Y. Ikemoto, T. Moriwaki, N. Yoneyama, M. Watanabe, A. Ueda, H. Mori, K. Kobayashi, R. Kumai, Y. Murakami, J. Müller, and T. Sasaki, *Science* **357**, 1381 (2017).
- [19] P. G. Debenedetti and F. H. Stillinger, *Nature (London)* **410**, 259 (2001).
- [20] C. A. Angell, *J. Non-Cryst. Solids* **131–133**, 13 (1991).
- [21] M. D. Ediger, *Annu. Rev. Phys. Chem.* **51**, 99 (2000).
- [22] H. Mori, S. Tanaka, and T. Mori, *Phys. Rev. B* **57**, 12023 (1998).
- [23] K. Kajita, Y. Nishio, S. Moriyama, W. Sasaki, R. Kato, H. Kobayashi, and A. Kobayashi, *Solid State Commun.* **64**, 1279 (1987).
- [24] H. Seo, *J. Phys. Soc. Jpn.* **69**, 805 (2000).
- [25] H. Seo, K. Tsutsui, M. Ogata, and J. Merino, *J. Phys. Soc. Jpn.* **75**, 114707 (2006).
- [26] M. Kaneko and M. Ogata, *J. Phys. Soc. Jpn.* **75**, 014710 (2006).
- [27] K. Yoshimi, M. Naka, and H. Seo, *J. Phys. Soc. Jpn.* **89**, 034003 (2020).
- [28] T. Mori, *J. Phys. Soc. Jpn.* **72**, 1469 (2003).
- [29] R. Kondo, M. Higa, S. Kagoshima, H. Hoshino, T. Mori, and H. Mori, *J. Phys. Soc. Jpn.* **75**, 044716 (2006).
- [30] M. Kobayashi and H. Tanaka, *J. Phys. Chem. B* **115**, 14077 (2011).
- [31] F. Nad, P. Monceau, and H. M. Yamamoto, *Phys. Rev. B* **76**, 205101 (2007).
- [32] Y. Nogami, N. Hanasaki, M. Watanabe, K. Yamamoto, T. Ito, N. Ikeda, H. Ohsumi, H. Toyokawa, Y. Noda, I. Terasaki, H. Mori, and T. Mori, *J. Phys. Soc. Jpn.* **79**, 044606 (2010).
- [33] F. Nad, P. Monceau, and H. M. Yamamoto, *J. Phys. Condens. Matter* **20**, 485211 (2008).
- [34] K. Suzuki, K. Yamamoto, K. Yakushi, and A. Kawamoto, *J. Phys. Soc. Jpn.* **74**, 2631 (2005).
- [35] T. Sato, K. Kitai, K. Miyagawa, M. Tamura, A. Ueda, H. Mori, and K. Kanoda, *Nat. Mater.* **18**, 229 (2019).
- [36] J. Merino, H. Seo, and M. Ogata, *Phys. Rev. B* **71**, 125111 (2005).
- [37] M. Tamura, H. Kuroda, S. Uji, H. Aoki, M. Tokumoto, A. G. Swanson, J. S. Brooks, C. C. Agosta, and S. T. Hannahs, *J. Phys. Soc. Jpn.* **63**, 615 (1994).
- [38] M. Dressel, *J. Phys. Condens. Matter* **23**, 293201 (2011).
- [39] K. Takenaka, M. Tamura, N. Tajima, H. Takagi, J. Nohara, and S. Sugai, *Phys. Rev. Lett.* **95**, 227801 (2005).
- [40] Y. Nakamura and S. Uchida, *Phys. Rev. B* **47**, 8369 (1993).
- [41] T. Valla, P. D. Johnson, Z. Yusof, B. Wells, Q. Li, S. M. Loureiro, R. J. Cava, M. Mikami, Y. Mori, M. Yoshimura, and T. Sasaki, *Nature (London)* **417**, 627 (2002).
- [42] N. Tajima, S. Sugawara, M. Tamura, Y. Nishio, and K. Kajita, *J. Phys. Soc. Jpn.* **75**, 051010 (2006).
- [43] D. Liu, K. Ishikawa, R. Takehara, K. Miyagawa, M. Tamura, and K. Kanoda, *Phys. Rev. Lett.* **116**, 226401 (2016).
- [44] M. Watanabe, Y. Nogami, K. Oshima, H. Mori, and S. Tanaka, *J. Phys. Soc. Jpn.* **68**, 2654 (1999).
- [45] T. Ito, M. Watanabe, K.-I. Yamamoto, N. Ikeda, Y. Nogami, Y. Noda, H. Mori, T. Mori, and I. Terasaki, *Europhys. Lett.* **84**, 26002 (2008).
- [46] M. Watanabe, Y. Noda, Y. Nogami, and H. Mori, *J. Phys. Soc. Jpn.* **73**, 116 (2004).
- [47] H. Watanabe and M. Ogata, *J. Phys. Soc. Jpn.* **75**, 063702 (2006).
- [48] M. Watanabe, Y. Noda, Y. Nogami, and H. Mori, *Synth. Met.* **135–136**, 665 (2003).
- [49] L. B. Ioffe and A. J. Millis, *Phys. Rev. B* **58**, 11631 (1998).
- [50] H. Taniguchi, Y. Nakazawa, and K. Kanoda, *Phys. Rev. B* **57**, 3623 (1998).
- [51] A. F. Ho and A. J. Schofield, *Phys. Rev. B* **71**, 045101 (2005).
- [52] K. Miyagawa, A. Kawamoto, and K. Kanoda, *Phys. Rev. B* **62**, R7679 (2000).
- [53] C. Hotta and N. Furukawa, *Phys. Rev. B* **74**, 193107 (2006).
- [54] M. Müller, P. Strack, and S. Sachdev, *Phys. Rev. A* **86**, 023604 (2012).
- [55] R. G. Palmer, D. L. Stein, E. Abrahams, and P. W. Anderson, *Phys. Rev. Lett.* **53**, 958 (1984).
- [56] K. Binder and P. A. Young, *Rev. Mod. Phys.* **58**, 801 (1986).